Wear 380-381 (2017) 146–153

Contents lists available at ScienceDirect

Wear

journal homepage: www.elsevier.com/locate/wear

Microstructural evolution in bearing steel under rolling contact fatigue

Shu-Xin Li [a,*], Yun-Shuai Su [b], Xue-Dao Shu [a], Jian-Jun Chen [a]

[a] School of Mechanical Engineering and Mechanics, Ningbo University, Ningbo 315211, PR China
[b] School of PetroChemical Engineering, Lanzhou University of Technology, Lanzhou 730050, PR China

ARTICLE INFO

Article history:
Received 1 January 2017
Received in revised form
21 March 2017
Accepted 21 March 2017
Available online 23 March 2017

Keywords:
Rolling contact fatigue (RCF)
White etching area (WEA)
Wear debris
Amorphization
Transformation

ABSTRACT

The purpose of this investigation was to study microstructural evolution leading to the formation of wear debris and white etching areas (WEA) in the subsurface of AISI 52100 steel during rolling contact fatigue (RCF). The specimens were tested using a roller-on-roller geometry testing machine. Surface damage was characterized using scanning electron microscopy (SEM) and transmission electron microscopy (TEM). Lamellar structures generated during the rubbing of crack faces give a clear picture of how wear debris is formed. In contrast to the previously reported WEA, which is composed of nano-ferrites generated under the mechanism of recrystallization, the WEA produced in the current RCF condition consists of an amorphous phase with nanocrystallites dispersed. Based on this, it is proposed that WEA can be classified into deformed WEA and transformed WEA depending on whether phase transformation occurs. In addition, the relationship between white etching crack (WEC) and WEA was discussed in detail. The result suggests that WEC does not initiate WEAs as it has been accepted. Instead, they form under different mechanisms.

© 2017 Elsevier B.V. All rights reserved.

1. Introduction

Bearings subjected to rolling contact fatigue (RCF) are often observed to fail in the way of pitting. When they are sectioned to expose interior microstructures, it is found that two distinct features exhibit: large number of cracks and microstructural alternation. Relative movement of crack faces can bring about change in the microstructure in the vicinity of cracks which leads to wear debris. Evidence has been given by Cvetkovski [1] to support that wear debris forms through wear and friction within crack faces rather than due to corrosion products or external contamination. This is supported by Matsunaga [2] who states that wear debris is generated by the microstructural change at the crack tip.

Apart from wear debris, some studies highlighted that the friction between crack faces can induce formation of WEA as a result of microstructural change [3,4]. These cracks are called as white etching cracks (WEC) correspondingly. This view is in contrast to the existing mechanisms such as hydrogen and nonmetallic inclusion induced, stress or sliding dominated WEA [5–12]. WEA is observed in both tempered martensite bearing steels [13] and carbide-free nano-sized bainite bearing steels [14], despite that the fact that the former is harder than the matrix while the latter is softer. The formation of WEA has been regarded as a potential damage of materials since it causes severe local inhomogeneity of microstructure in RCF. However, the key issue is: can the rubbing of crack faces cause microstructural change which leads to the formation of WEA? Although extensive studies have been carried out, the rubbing process of crack faces and microstructural evolution in the subsurface of RCF are still not well understood.

The remarkably sheared morphology of WEA and elongated carbides indicate that materials are subjected to large plastic deformation in RCF [15,16]. Such a severe deformation can induce either refined microstructure or a phase transformed microstructure, thus creating deformed or transformed shear band correspondingly [17]. The sheared morphology of WEA mainly consists of body-centred cubic nano-sized ferrites [5,15] despite that, an amorphous-like structure was inspected inside of WEA by Harada et al. [18] and later by Evans [19]. However, the formation of WEA is highly dependent on loading parameters. Various WEAs can be generated under different RCF loading and contact conditions. Hereby, a question is raised that in addition to the WEA of refined grains (nanocrystallites), is it possible that a new type of WEA of phase transformation exists? If so, what is the final product and what is the difference from the reported WEA? This issue has never been reported so far.

With these questions, the current study conducted RCF tests to produce WEA. Microstructural evolution in terms of formation of wear debris and WEA were investigated. Emphasis was placed on composition and formation mechanism of WEA with an attempt to have a clear understanding of how WEA forms in RCF. The

* Corresponding author.
E-mail address: li_shuxin@163.com (S.-X. Li).

http://dx.doi.org/10.1016/j.wear.2017.03.018
0043-1648/© 2017 Elsevier B.V. All rights reserved.

relationship between WEA and WEC was discussed in detail in order to clarify whether WEC is a prerequisite of WEA formation.

2. Materials and methods

The material used for RCF tests is a tempered martensitic steel AISI 52100. The chemical composition is as follows (wt.%): C, 0.90; Cr, 1.87; Si, 0.31; Mn, 0.32; P, $\leq$ 0.027; S, $\leq$ 0.020. Fe, balance. Samples were austenitized at 860°C for 2 h, followed by quenching in oil to room temperature, and tempered at 160 °C for 1 h. The final hardness is 58 HRC.

The rolling contact fatigue test was carried out under lubrication on a two-roller machine. The lubricant used was PAG gear oil, viscosity grade 68 gear oil with the kinematic viscosity at 40 °C of 68.7 mm^2/s, the viscosity index of 175 and the flash point of 242 °C. Both rollers are made of the same material. The upper roller has a crown of 60 mm in diameter and 5 mm in width and the lower roller of the same diameter of 60mm, as shown in Fig. 1. Each roller is driven by a separate motor, allowing for variation in slide-to roll ratios (SRRs). SRR is defined as the difference of the upper and lower surface velocities divided by the mean value of surface velocity [20].

The maximum Hertzian contact pressure of 0.9 GPa to 2.0 GPa and the SRRs of 5% to 20% were employed to generate various WEA. The tests were stopped when the vibration of the machine is beyond the critical value due to the presence of macro pits in the surface. The failed samples of upper roller were sectioned both circumferentially and axially and then polished and etched in 2% nital etchant for microstructural inspections. Both SEM and TEM inspections were conducted. The TEM foil sample of interest was cut by Focused Ion Beam (FIB).

3. Results

3.1. Development of surface pitting

Fig. 2 shows the surface morphologies at various damage stages of RCF under 1.2 GPa and SSR of 10%, with the RCF life of 3.1×10^6 cycles. The development of surface pitting can be observed in them. Circular micropits were generated in the peaks which have been flattened and valleys of the surface roughness in Fig. 2(a). As the RCF proceeded, transverse microcracks formed at micropits and coalesced with neighbouring microcracks, which leads to clusters of microcracks as shown in Fig. 2(b). Also, newly-formed micropits appeared simultaneously. When this cyclic process continued, micropits and microcracks grew and eventually linked up into networks, resulting in spalling of materials in Fig. 2(c).

3.2. Formation of lamellar structures

Fig. 3 shows observations on repetitious rubbing of crack faces in the subsurface of RCF. Microstructure inside of the crack was substantially elongated along the shear direction and interior cracks were generated in Fig. 3(a). A distinctive feature are lamellar structures that degraded into small lamellar flakes through the rubbing of surface faces. They layered and tended to have the same orientations as shown in Fig. 3(b) and (c), where a number of lamellar flakes with thickness ranging from 0.2 μm to 1.2 μm layered in a regular way. It can be inferred that as the repetitious rubbing and shear deformation continues, these lamellar structures will be rubbed into even smaller particles, forming wear debris eventually. The energy dispersive X-ray (EDX) inspection shows that the wear debris at the points 1–6 in Fig. 3(b)-(d) have the identical compositions. Table 1 lists the chemical compositions.

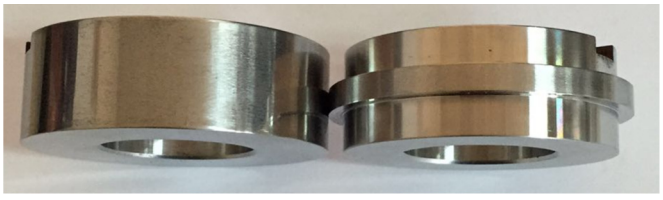

Fig. 1. Photo of the sample in RCF.

Apart from the regular lamellar structures, twisted and rotated microstructures were also observed as marked in Fig. 3(d), which indicates that out-of-plane shear stress works on refining microstructures. In addition, some wear debris were debonded directly from the crack face as arrowed in Fig. 3(d). We repeated the inspections with different samples and found a similar microstructural evolution. The rubbing of crack faces is evidenced by the striations left on the crack faces during repetitious contact and friction in Fig. 3(e), which is the typical feature of fatigue crack propagation.

3.3. Microstructure of the WEA

WEAs were generated at depths 0.5–1.0 mm away from the contact surface of RCF. WECs were observed to form either inside or at the edge of the WEA. It is hard to follow in what cracks and in which part of them WEA can form as cracks exhibit much scatter in terms of locations and orientations with respect to the subsurface. The answer has to depend on large number of inspections of sectioned samples. Fig. 4 displays a typical crack morphology under SEM. The crack is located in the depth of 810 μm from the surface. The well-developed WEA exhibits a totally different structure from the matrix. The width of the WEA varies along the crack. In addition to a main WEC which goes through the interior of the WEA along the shear direction, some small cracks were generated as well. They split the WEA into segments with the widest WEA of 2.6 μm on the left side. Apart from small partitioned WEAs, wear debris can be seen inside of cracks.

Fig. 5 displays the TEM sample preparation by FIB. The WEA is in-between the matrix as marked by the two dotted lines. WECs go deep into the thickness. The carbides can be clearly seen on the left and right hand side of the matrix, but no carbides are present in the WEA. The EDX analysis in Fig. 6 shows that when crossing the interface, there is no significant difference in the element composition except for Fe, which has a slight increase respectively.

Fig. 7 displays the bright field TEM microstructures and the high resolution TEM (HRTEM) micrographs. The interface between the matrix and the WEA can be clearly seen in Fig. 7(a). Grains were elongated along the shear direction in the matrix. Large amounts of dislocation clusters were observed and some nano grains less than 100 nm formed as shown in Fig. 6(b). The selected area diffraction (SAD) at the place B in Fig. 7(b) shows that the matrix was largely deformed, but carbides remained undeformed as indicated by the SAD of "A". In contrast, no grains were observed in the WEA at this magnification and it presents an amorphous state. At a higher magnification in Fig. 7(c), some black particles with an average size of 5 nm and grey microstructure can be clearly seen. The SAD indicates an amorphous phase but with some nanocrystallites embedded. Further inspections of HRTEM in Fig. 7 (d) show that the grey microstructure tends to be amorphous, while the black particles present nanocrystallites.

4. Discussion

4.1. Formation of wear debris

Lamellar structures consisting of layers of sheared flakes are formed in between the crack, as shown in Fig. 3. The cyclic contact

Download English Version:

https://daneshyari.com/en/article/4986500

Download Persian Version:

https://daneshyari.com/article/4986500

Daneshyari.com